Pergamon

Phys. Chem. Earth (B), Vol. 25, No. 9, pp. 757–763, 2000

1464-1909/00/$ - see front matter

PII: S1464-1909(00)00098-8

Numerical Simulation of Real Debris-Flow Events

L. Fraccarollo[1] and M. Papa[2]

[1]Ass. Professor, University of Messina, Contrada Sperone 31, 98166 S. Agata, Messina, Italy
[2]Postgraduate student, University of Bologna, viale Risorgimento 1, 40136 Bologna, Italy

Received 29 July 1999; accepted 18 December 1999

Abstract. A one-dimensional model is presented to predict debris-flow runouts. The model is based on shallow water type assumptions. The fluid is assumed to be homogeneous and the original bed of the flow domain to be unerodible. The fluid is characterized by a rheology of Bingham type.

A numerical tool able to cope with the nature of debris flows has been worked out. It represents an extension of a second order accurate and conservative method of Godunov type. Special care has been devoted to the influence of the source terms and of the geometrical representation of the natural cross sections, which play a fundamental role.

The application concerns a monitored event in the Dolomites in Italy, where field analyses allowed a characterization of the behavior of solid-liquid mixture as a yield stress material. The comparison between numerical simulations and field observations highlights the impossibility of representing all phases of the flow with constant values of the rheological parameters. Nevertheless the results show that it is possible to separately represent the phase of the flow in the upstream reach and the phase of the deposition in the alluvial fan, with a good agreement with field observations.

1 Introduction

The approach to numerical modeling of debris flows must take into account the nature of the flowing material, constituted of a mixture of water and sediments, and the nature of the flow itself, which is unsteady and includes steep fronts.

A liquid phase and a solid phase form the flowing material. The liquid phase is made up of water and of the finer grain fractions, while the solid phase is made up by the coarser grain fractions. In debris flow modeling two different approaches are possible: two phases (or multi-phases) model, and single-phase model.

Correspondence to: Maria Papa

A two-phase model treats separately the solids and the fluid. When the hypothesis that there is no relative velocity between the two phases applies, the resulting integrated model presents only one momentum equation, derived for a fluid with the bulk density. The equations, which describe the flow, are completed by a mass conservation equation for each of the two phases. This scheme permits a non-homogeneous treatment of the mixture. It is able to simulate the entrainment and deposition processes through the movable bottom line, and, therefore, is suitable to face problems where the morphological evolution is to be determined. Zanré and Needham (1996), Hungr (1995), Lai (1991), Morris and Williams (1996) inspired their works from this model.

Situations with no significant morphological changes often take place. In these cases it is possible to consider the mixture as a homogeneous and single phase. The resulting integrated models present only the volume conservation equation and the momentum equation, derived for a fluid with the bulk mass density. Only a closure relation relevant to the rigid-bottom shear stress is necessary, whereas the non-homogeneous-fluid model requires the local transport capacity relationship as well. The channel morphology is assigned. Despite the bed is unerodible, the simulation of stopping processes is still possible when the constitutive equation for the bottom shear stress includes a yield stress, as for Herschel-Bulkley fluids, Bingham fluids, and so on. In deed, there are many field and experimental observations of flow behaviors of this kind, as reported in Coussot (1994) and Whipple (1997), among others.

In dealing with simulations of flows an important issue concerns the choice of the appropriate dimensional frame in which they may be represented. A three-dimensional model, given by Navier Stokes equation type, is applicable only to local situations because of computing time and hardware resources required.

Usually debris flows can be considered as shallow water flows, which means that the flow depth is small compared to the length of the channel. Consequently, following the De Saint-Venant approach, local variables can be integrated along the vertical direction obtaining a two-dimensional model, or over the cross-section, obtaining a one-dimensional model. The two-dimensional models are suitable to model the open boundary case such as not channelled flows and alluvial fans (Fraccarollo, 1996). Friction effects along the bed and the banks, and the stress between inner adjacent columns of fluid are not known, thus they require assumptions for their computation.

The one-dimensional models properly represent channelled flows and possible overtopping condition. In this case the overall contribution of the shear stress on the rigid boundary is locally provided in analogy with the case of a uniform flow having the same depth and mean velocity.

The present work deals with applications to real debris flows involving a fluid with a not negligible fine content, running down inside a channel. This is the reason why, in this paper, we restricted our attention to a one-dimensional model of a homogeneous fluid. The need to simulate real debris flows puts stiff problems in the treatment of the fluxes and of the source terms in the momentum balance. The difficulties arise from the deviations from the pure conservation form of the momentum equation and from the need to detect the stopping of the flow with accuracy both in time and in space. Furthermore, in real debris-flow events, the knowledge of the rheological parameters are much more important than in sediment transport or in clear water cases, and much more difficult to be determined in the field, too. The paper presents a numerical model where these problems have been faced and a solution is proposed.

2 The mathematical and numerical modelling

In the one-dimensional case the De Saint Venant equations are:

$$\frac{\partial(S)}{\partial t}+\frac{\partial(US)}{\partial x}=0 \tag{1}$$

$$\frac{\partial(US)}{\partial t}+\frac{\partial(\beta UUS)}{\partial x}+kg\,S\cos\theta\;\frac{\partial(h)}{\partial x}= \\ =g\,S\,(\sin\theta-i_E) \tag{2}$$

where x is the distance along channel axis, t is the time, θ is the channel slope, U is the flow velocity, h is the depth of flow, g is the gravity, S is the cross section area, i_E is the energy-line grade, k is the earth pressure coefficient and β is the momentum coefficient. In the applications k and β will be assumed equal to 1.

The numerical strategy here employed has taken into account the main features of the debris flows, that include steep fronts and discontinuities of the free surface. Moreover, when a Bingham-type threshold in the constitutive relationship is present, the flow may locally stop and restart, even over steep slopes.

The influence of such a morphology and fluid rheology on the flow removes the possibility to employ simplified models such as the kinematic model, and makes the use of conservative methods necessary.

In case that the width at the free-surface level depends on the longitudinal position and on the flow depth, this purely geometrical character affects all the fluxes in the balances equations. A further problem arises also from being the last term in the momentum flux (Eq. (2)) not conservative anymore. The loss of conservation is a major point in the numerics, and requires special care. It is also true that the resulting system of equations is equivalent to the following one, written in an rearranged non conservative form, when no discontinuities at the free surface occur:

$$\frac{\partial(S)}{\partial t}+\frac{\partial(US)}{\partial x}=0 \tag{3}$$

$$\frac{\partial(U)}{\partial t}+U\frac{\partial(\beta U)}{\partial x}+kg\cos\theta\;\frac{\partial(h)}{\partial x}=g\,(\sin\theta-i_E) \tag{4}$$

From these equations we may infer that the geometrical characterisation of the channel shape is still present only in the continuity equation. This fact suggests that keeping the shape effects in the momentum equation is important only when discontinuities have to be computed. After this observation, it is possible to build a Godunov type method based on the solution of local Riemann problems relevant to the following system of equations in conservative form:

$$\frac{\partial(\mathbf{U})}{\partial t}+\frac{\partial(\mathbf{F})}{\partial x}=0 \tag{5}$$

where $\boldsymbol{U}$ and $\boldsymbol{F}$ are, respectively, the vectors of the state variables and of the fluxes, to be now specified. The Riemann-problem solutions contribute, as herein clarified, to the evaluation of the numerical fluxes $\boldsymbol{F}$ in Eq.(5). Following the above reported observation, we based the Riemann-problem solutions on Eq.(3) and on the following one for the momentum balance, both written in a conservative way:

$$\frac{\partial(hU)}{\partial t}+\frac{\partial(\beta hUU)}{\partial x}+g\;\;k\,\frac{\partial(h^2\cos\theta)}{\partial x}=0 \tag{6}$$

The first step of the method is relevant to the solution of the local Riemann problems defined at the spatial boundary between two adjacent grid cell. It is achieved by using the approximate HLL solver (Harten et al., 1983), whose advantages dwell in its simplicity and robustness (Fraccarollo and Toro, 1995). The solution of the Riemann problem consists in determining the speed and the type of the two bounding waves, the left one E_L and the right one E_R, and the flux vector $\boldsymbol{F}^*$ in the central region of the wave structure, where the variables are constant. The wave speeds E_L and E_R are estimated as the values given by the two-rarefaction approximation (Toro, 1992), here corrected to take into account the effect of the slope, of the section shape, and of the non newtonian rheology of the fluid:

$$E_L = \beta U - \sqrt{kgh\cos(\theta)};\quad E_R = \beta U + \sqrt{kgh\cos(\theta)} \tag{7}$$

The HLL approximation provides the following direct solution for the intercell flux vector F^* at the boundary $x_{i+1/2}$, depending on the initial values at the left side (position i) and at the right side (position $i+1$):

$$\boldsymbol{F}^*_{i+1/2} = \frac{E_L \boldsymbol{F}_{i+1} - E_R \boldsymbol{F}_i + E_L E_R (\boldsymbol{U}_{i+1} - \boldsymbol{U}_i)}{E_R - E_L} \tag{8}$$

The HLL approximation also provides the state of variables $\boldsymbol{U}^*$ in the star state, as a result of the following expression:

$$\boldsymbol{U}^*_{i+1/2} = \frac{E_R \boldsymbol{U}_{i+1} - E_L \boldsymbol{U}_i + \boldsymbol{F}_i - \boldsymbol{F}_{i+1}}{E_R - E_L} \tag{9}$$

These equations are not redundant in the evaluation of the fluxes, because of the approximation we introduce in the choice of the waves. Based on our experience on shallow water equations (Fraccarollo and Toro, 1995), we use Eq.(8) for the continuity equation (Eq.(3)), whereas Eq.(9) is applied to both continuity and momentum equation (6)), in order to obtain the flow depth h^* and the velocity u^* in the star state: these two primitive variables are necessary to evaluate the momentum fluxes in Eq.(2). The second order in time and space WAF method (Toro, 1992) is then applied. It consists in a determination of the numerical intercell fluxes, at the position $i+1/2$, as the average of the Riemann fluxes, over the distance (x_i, x_{i+1}), and at the time $t=t^n+\Delta t/2$ (where t^n is the present time with the variables already updated, and Δt is the numerical time step). Any necessary information for this flux average is available and readily applicable.

Before deploying the final conservation laws it is necessary to show the treatment of the cross-section area. In case of a rectangular section $S=Bh$, where B is the width, generally variable along the channel. We may rewrite the non conservative part of the momentum flux as follows:

$$g\frac{B}{2}\cos\theta\frac{\partial h^2}{\partial x} \tag{10}$$

By doing so, when B is constant, this flux is automatically free-divergent. In the general case of a non rectangular shape of the cross section, we adopt the following equivalence:

$$S = w(h)h \tag{11}$$

and then we may still employ Eq.(10), where B is replaced by w, which, for a general section, is an assigned function of the flow depth h. Using, by instance, a trapezoidal section, it comes out that $w=b+sh/2$, being s the sum of the two bank cotangents and b the basal width. The equivalent width w depends now also on the flow depth.

The area S in each grid-cell is updated by means of the continuity equation as it follows:

$$(S)_i^{n+1} = (S)_i^n - \frac{\Delta t}{\Delta x}\left[(US)_{i+1/2}^{WAF} - (US)_{i-1/2}^{WAF}\right] \tag{12}$$

from which the flow depth at the new time-step is also available.

The momentum equation (Eq.(2)) is now considered. Because of the presence of a non conservative term in the fluxes, we use the values h^* and u^*, calculated as shown above, to calculate separately the conservative and the non conservative flux, obtaining the WAF evaluation of (βUUh) and of $(kg/2\ h^2 \cos\theta)$, respectively. Finally, the time integration of Eq.(2) is obtained by the following relationship:

$$(US)_i^{n+1} = (US)_i^n - \frac{\Delta t}{\Delta x}\left[(\beta UUwh)_{i+1/2}^{WAF} - (\beta UUwh)_{i-1/2}^{WAF}\right] - \\ - w_i^{n+1}\frac{\Delta t}{\Delta x}\frac{1}{2}gk\left[(h^2)_{i+1/2}^{WAF} - (h^2)_{i-1/2}^{WAF}\right]\cos\theta \tag{13}$$

In the final step the computation treats the source terms in the momentum equation, which are so important in debris flows. Subsequent Chapter 3 is devoted to this issue.

3 Source terms and closure relations

The source terms are particularly important in debris flows, also under the hypothesis of an homogeneous fluid. They take into account the shear stress on the rigid boundary and the slope of the bottom profile. They are both remarkably higher than in clear-water flows.

As far as the averaged shear stress on the rigid boundaries is concerned, we consider here the problem of the representation of uniform flow relationships for a Bingham fluid. The velocity distribution has to be calculated as the solution of an elliptic differential system of equations, based on the conservation of mass and momentum and generalized Bingham constitutive law, with appropriate boundary conditions. The analytical solution for the non dimensional

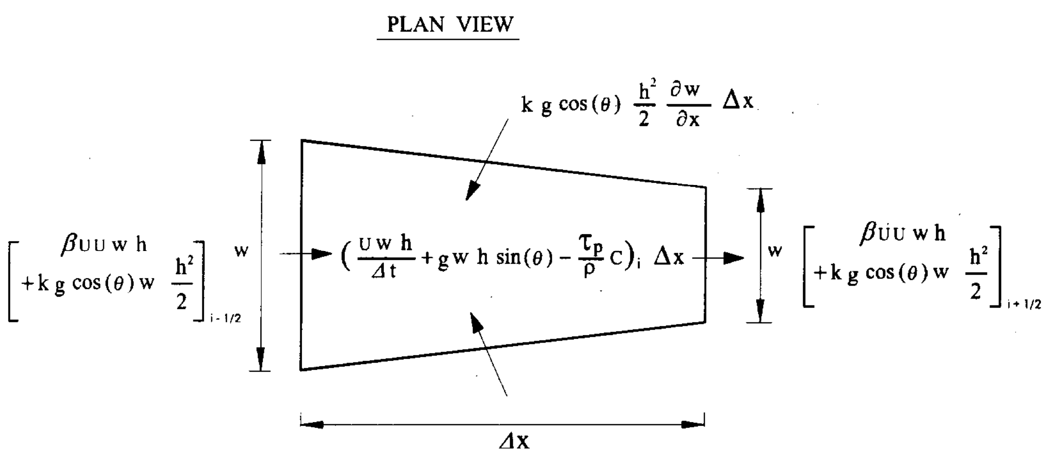

Fig.1. Schematic representation of forces acting on a one-dimensional cell. Arrows crossing the cell boundaries represent the momentum fluxes.

discharge through an infinitely wide channel is (Johnson, 1970):

$$\frac{Q\cdot\mu}{\gamma\cdot i_E\cdot W\cdot H^3}=\xi\left(\frac{\tau_0}{\tau_{\lim}}\right) \tag{14}$$

where Q is the discharge, μ the Bingham viscosity, γ the mixture unit weight, i_E the energy gradient, W the flow width at the free surface, H the flow depth at cross section centre. The discharge is related to the non-dimensional term ξ that is a function of the ratio between the yield strength (τ_0) and the critical shear stress (τ_{lim}). The critical shear stress, that is defined as the maximum yield strength at which flow is possible, is a property of channel geometry and of acting forces. In the case of an infinitely wide channel, critical shear stress is equal to $\gamma\ H\ \sin\theta$. The condition that applies at the transition between quiet condition and motion, or vice-versa, is $\tau_{lim}=\tau_0$, that gives ξ equal to zero.

When the hypothesis of large rectangular section is not applicable, the location of the plug boundary and therefore the critical shear stress is not known a priori. The solution of uniform flow relationships may not be produced in an analytical way. The methodology here developed exploits the results obtained by Whipple (1997). He provided numerical solutions by using a commercially available finite-element code (FIDAP). A regression analysis of the model results provided general equations. The domain portion interested by the maximum-velocity plug does not occupy the whole width, and also zero-velocity plugs may appear, as those in the low corners of trapezoidal and triangular sections. Results by Whipple are proposed as it follows:

$$\frac{Q\cdot\mu}{\gamma\cdot i_E\cdot W\cdot H^3}=\psi_1\left(\frac{W}{H}\right)\xi\left(\frac{\tau_0}{\tau_{\lim}}\right) \tag{15}$$

$$\frac{\tau_{\lim}}{\gamma H \sin\theta}=\psi_2\left(\frac{W}{H}\right) \tag{16}$$

The dimensionless parameters ψ_1 and ψ_2 take into account the ratio W/H. The results of Whipple analyses provide the expression of the terms ψ_1, ψ_2 and ξ for some, among the most common, section shapes.

From inverting Eq.(15) it is possible to compute the energy gradient (i_E) as a function of the state variable H and Q, and then the average boundary shear stress ($\tau_p=\gamma{\cdot}R_h{\cdot}i_E$, where R_H is the hydraulic radius).

The average strength τ_p acting on the section boundary in stopping conditions ($\tau_{lim}=\tau_0$) can be obtained by Eq.(16); we may finally use the following expression:

$$\tau_p=\frac{\tau_0}{\Psi_2}\frac{R_h}{H} \tag{17}$$

4 Local flow stop and restart

The skill of the model to reproduce the mechanism of arrest and restart of the flow is fundamental in debris flow simulations. The possibility to model the rest conditions of the fluid over slopes is provided by the presence of a cohesive-type stress. The presence of a yield stress has also a strong implication in the numerical strategy. In the present method, we exploit its being explicit in order to guarantee a sharp determination of the stop conditions in time and space. The time-step is subjected to a Courant type restriction for the stability. Figure1 shows the balance of forces that are locally applied in a numerical cell before marching in time to the subsequent time-level. These forces represent each term of the momentum equation (Eq.(2)).

The numerical fluxes are already determined from the solutions of the Riemann problems on the basis of the state-variable distribution available at the previous (old) time level. It is to be noted that the pre-determination of the inertia force ($whU/\Delta t$), which aids the motion, is under-sized when the flow is actually going to stop in less than the time-step Δt, while is over-sized when no local stop will take place. Therefore, the prediction is always not biased by under- over-estimation of the inertia. When the modulus of the algebraic sum of all the forces acting on the cell mass or on the cell boundaries exceeds the product ($\tau_p\ c\ \Delta x$), where c is the wetted perimeter of the section, the flow will not stop during the present time-step.

5 Application to Acquabona catchement

The Acquabona catchement is located on the left side of Boite Valley, near Cortina D'Ampezzo (Italy), where debris flows occur almost every year. Along the channel, a monitoring system has been set up (Berti et al., 1999). An ultra sound Doppler system allows the measurement of the flow depth in time while an estimation of the average front velocity is obtained by using a set of three geophones. Registrations of two events happened on June 12th 1997 and on August 17th 1998 are available.

Grain size distribution analyses (Berti et al., 1999), on material sampled at Acquabona site, showed that the finer fraction (silt and clay) is about 10% in the upper part of the channel and about 30% in the deposit area. The amount of the finer fractions suggests a global rheological behavior of visco-plastic type (Coussot, 1994; Whipple, 1997).

5.1 Rheological parameters

In the applications, the rheological parameters are supposed to be constant along the channel and in time.

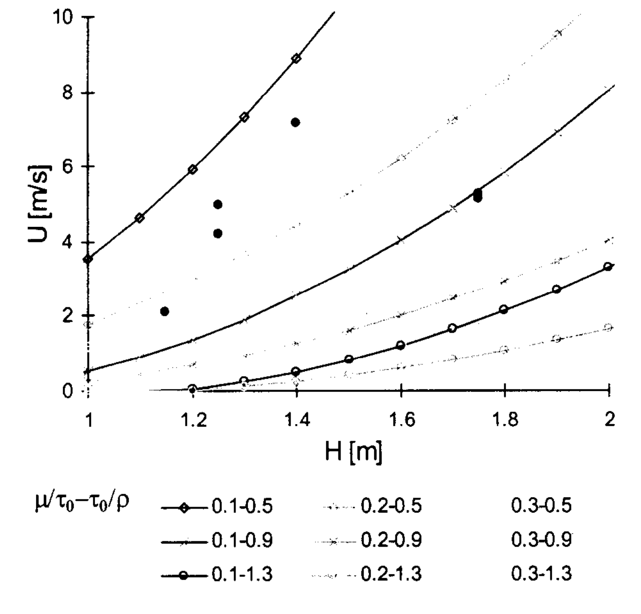

Fig.2. Comparison between Whipple flow equation and field observations.

A field evaluation of the yield stress is given by the equilibrium of uniformly deposited layers:

$$\frac{\tau_0}{\rho} = g h_d \sin\theta_d \tag{18}$$

where h_d is the depth of the deposit, observed to be equal to about 1 m; and θ_d is the bed slope angle in the deposition area, whose average value is equal to 7.8°. The resulting value is $\tau_0/\rho = 1.3\ m^2/s^2$.

The depths and the velocities of the flow, measured in the channel upstream the deposit area, during the last monitored event, are reported in Fig.2. The relations between velocity and depth of flow proposed by Whipple (Eq.(15)) are reported in the same figure with different values of the rheological parameters. It may be inferred that the value of the yield shear stress better representing the stopping condition is sensibly different to the one representing the dynamic of the flow in the upper part of the channel. For this reason the simulations have been carried out with two different sets of rheological parameters. For the calibration of the flow upstream the deposit area, the set (a) has been used:

$$\text{set(a)} \qquad \frac{\mu}{\tau_0} = 0.1\ s \qquad \frac{\tau_0}{\rho_m} = 0.5\ m^2/s^2 \tag{19}$$

While for the calibration in the stopping conditions, the set (b) has been used:

$$\text{set(b)} \qquad \frac{\mu}{\tau_0} = 0.1\ s \qquad \frac{\tau_0}{\rho_m} = 1.3\ m^2/s^2 \tag{20}$$

5.2 Comparison between field data and simulations results

As showed in Fig.3, the stage hydrographs given by field observations show significant fluctuations.

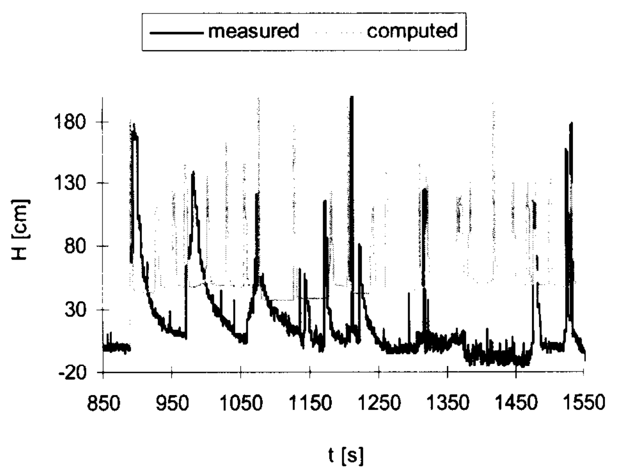

Fig.3. Comparison between depth of flow, measured and calculated with the set of parameters (a).

The set *(a)* of parameters has been used to simulate the formation and propagation of the debris waves. The numerical model is able to represent, in a qualitative way, the fluctuations of the flow that have been observed. The time of occurrence of the computed peaks and their wavelengths do not correspond to those observed, but heights of the peaks are well represented (Fig.3). This latter feature is relevant in dealing with the estimation of possible overflowing, which is one of the most important information for practical purposes. In the computed hydrograph the depth of flow cannot be less than the value determined by the presence of the yield strength in the rheological characterization of the flow. On the contrary the form of the measured hydrograph suggests that, in this part of the channel, the flow is not of the yield type.

As far as the downstream stopping process is concerned, it has been found that it can not be represented by the same set *(a)* of parameters, since what observed is that the debris keeps flowing beyond the actual deposit basin.

Using the set *(b)* of parameters the simulation of the depth and the spread of the deposit agrees with the observations, even though there is no evidence of the free-surface oscillations (Fig.4).

An analysis of the linear stability for a visco-plastic fluid (Trowbridge, 1987; Coussot, 1994) has demonstrated that free surface flows, of a fluid with large yield stress, is susceptible to instability at Froude numbers ($Fr = U/\sqrt{gH\cos\theta}$) greater than a critical value. The value of this critical Froude number is found to be less than 0.25.

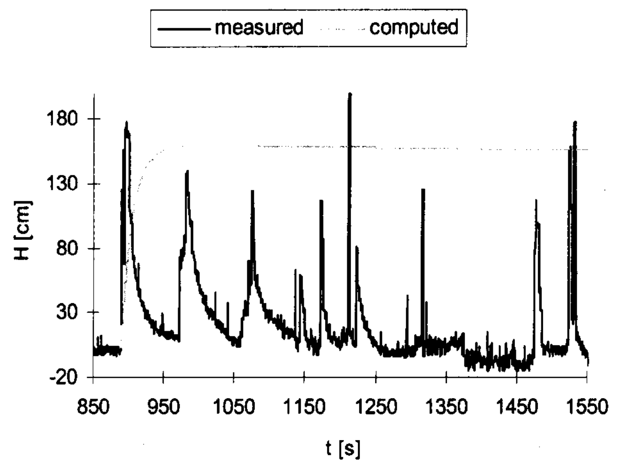

Fig.4. Comparison between depth of flow, measured and calculated with the set of parameters (b).

In Fig.5 this stability criteria is compared with field observation; the curve relevant to Fr=1, is also reported. The field measurements clearly show that the theoretical critical Froude number is always overtaken, substantiating the formation of the observed and calculated debris waves.

The graphic in Fig.6 shows the computed maximum depth reached in each section of the channel and the corresponding measurements derived from the trace left by the flow along the channel (Berti et al., 1999), for both the sets of the employed rheological parameters.

Results referring to the use of set b) of the rheological parameters determine a good representation of the deposition phase, even though there is an under-estimation of the maximum flow depth in the upstream channel. On the contrary, set a) produces a better simulation of the flow in the channel, where the impulsive waves are captured.

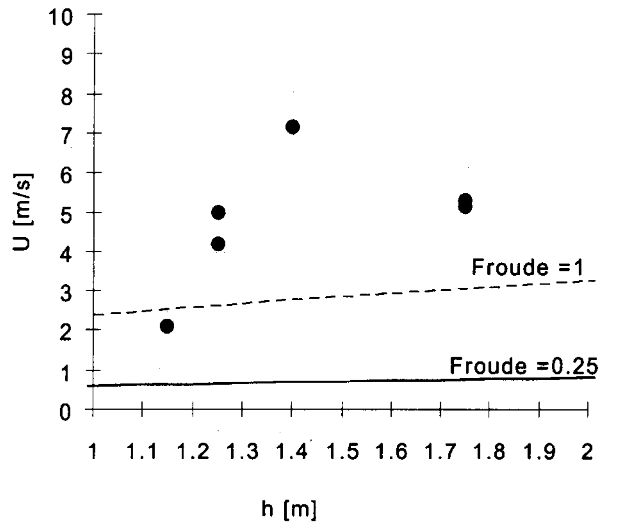

Fig.5. Comparison between field measurement and the critical Froude number.

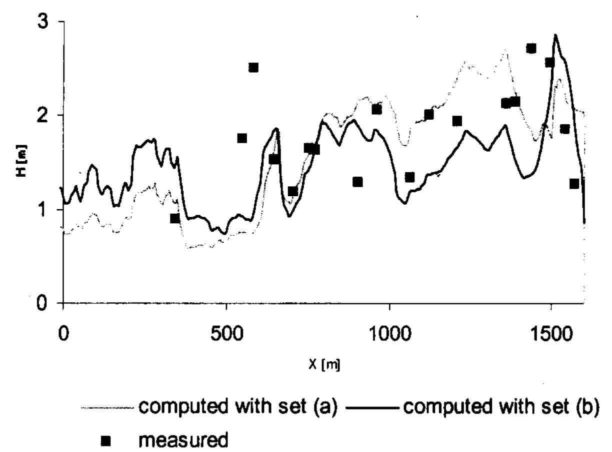

Fig.6. Comparison between the maximum depths of flow measured and calculated along the channel.

6 Conclusions

The objective of this work was the construction of a numerical tool able to reproduce the flooding waves of water and debris with considerable content of fine particles, and the deposition of the material in the alluvial fans. Attention has been paid to the effects induced by the not regular geometry of the natural channels, efforts has been made to keep as much as of the conservation in both volume and momentum balances, thus allowing a reliable representation of the impulsive behavior of the phenomenon. Furthermore, the stopping mechanism and the treatment of the source terms have been solved in a robust way.

The results of this study show that it is possible to represent all the phases of the flow, i.e. the debris waves in the intermediate part of the channel and the deposition process in the final reach of the basin, by using different sets of the rheological parameters. Time and space dependence of the rheological parameters may be linked to the nature of the phenomenon, where stone abrasion, outcropping of materials with the same or different characteristics in the flow, loss of water content, happen. All these aspects should be taken into account in the rheological definition of the fluid in order to increase the potentiality of the method and the accuracy of the results.

Acknowledgments. This work is a part of the EC Research Programme Environment and Climate 1994-1998, *Debris flow management and risk assessment in the alpine region*, Co-sponsored by Commission of the European Union DG XII with Contract ENV4-CT96-0253. The research director Prof. A. Lamberti is gratefully acknowledged for guidance and support.

References

Archetti, R., and Armanini, A., and Fraccarollo, L., and Laigle, D., and Lamberti, A., and Papa, M., Mathematical Modelling and Risk Assessment, DFR, final report, vol.1, EC Research Programme, ENV4-CT-0253, 1999.

Berti, M., and Genevois, R., and Ghirotti, M., and Simoni, A., and Tecca, P.R., Debris flow monitoring and analysis in the dolomitic region (upper Boite Valley, Italian Alps), DFR, final report, vol.2, EC Research Programme, ENV4-CT-0253, 1999.

Coussot, P., Lois d'ecoulement des laves torrentielles boueuses, *La Houille Blanche n°3*, pp.38-43, 1994.

Fraccarollo, L. and Toro, E. F., Experimental and numerical assessment of the shallow water model for two-dimensional dam-break type problems, *J. of Hyd. Res., vol.33, n°6*, 1995.

Fraccarollo, L., A simplified approach to debris flow simulation, Proc. XI International Conference on Computational Methods in Water Resources, Cancun, Mexico, 1996.

LAI, C., Modelling alluvial channel flow by multimode characteristic method. *J. Hydr. Engng 117*, 32-53, 1991.

Harten, A.., and Lax, P. D., and Van Leer, B., On upstream differencing and Godunov-type schemes for hyperbolic conservation laws, *SIAM Review, n° 25*, pp. 35-61.

HUNGR, O., A model for the runout analysis of rapid flow slides, debris flows, and avalanches. *Can. Geotech. J. 32*, 610-623, 1995.

Morris, P. H., and Williams, D. J. 1996 Relative celerities of mobile bed flows with finite solid concentration. *J. Hydr. Engng 122*, 311-315.

Jonson, A. M., *Physical Processes in Geology*. San Francisco, California, Freeman, Cooper & Co., 577p., 1970.

Toro, E. F., Rieman problems and WAF method for solving the two-dimensional shallow water equations, *Phil. Trans. R. Soc. London, 338*, pag.43-68, 1992.

Trowbridge, J. H., Instability of concentrated free surface flow, *Journal of geophysical research, vol. 92, n°c9*, pp 9523-9530, 1987.

Whipple, K.X., Open channel flow of Bingham Fluids: applications on debris flow research, *Journal of geology*, 1997

Zanré, D. D. L., and Needham, D. J., On simple waves and weak shock theory for the equations of alluvial river hydraulics. *Philos. Trans. Roy. Soc. A 354*, 2993-3054, 1996 .